Electronic Supplementary Material (ESI) for Nanoscale.

Effect of Aromatic Substituents in H-Bonded Assembly of Diketopyrrolopyrroles at Solid-Liquid Interfaces

Navathej Preetha Genesh,[a] Dominik Dettmann,[a,b] Daling Cui,[c] Yuxuan Che,[c] Violeta Toader,[c] Tarnjit Kaur Johal,[a] Chaoying Fu,[d*] Dmytro F. Perepichka,[c*] and Federico Rosei[a*]

a) Centre Énergie, Matériaux et Télécommunications, Institut National de la Recherche Scientifique, 1650 Boulevard Lionel-Boulet, Varennes, Québec J3X 1P7, Canada
b) Istituto di Struttura della Materia, Consiglio Nazionale delle Ricerche, via Fosso del Cavaliere 100, 00133 Roma, Italy
c) Department of Chemistry, McGill University, 801 Sherbrooke Street West, Montreal, Québec H3A 0B8, Canada
d) Huzhou Key Laboratory of Medical and Environmental Applications Technologies, School of Life Sciences, Huzhou University, Huzhou 313000, China

1) Molecular model of DSeDPP phase II

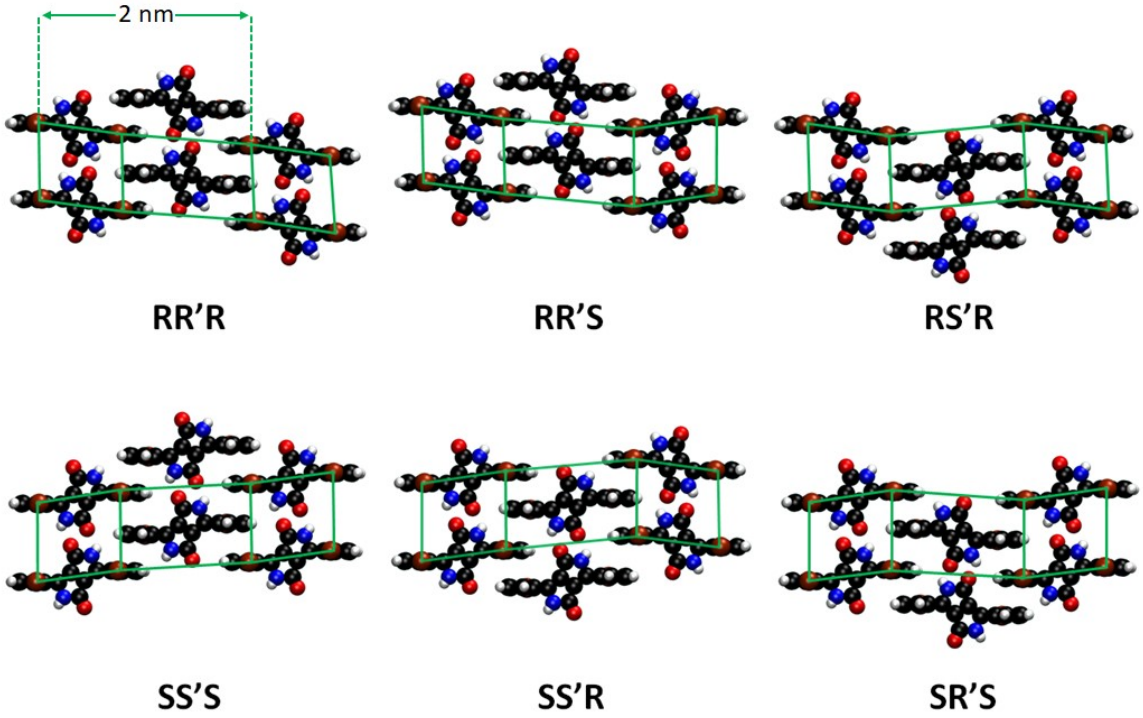

Figure S1. Molecular models showing possible diastereomeric trimers in the polymorph II of DSeDPP, where R' and S' correspond to the diastereomers with Se atoms facing down. Since the bright features in the STM image of phase II are attributed to protruding Se atoms, parallelogram grids (in green) are constructed by joining such Se atoms for easy interpretation.

2) Additional STM images

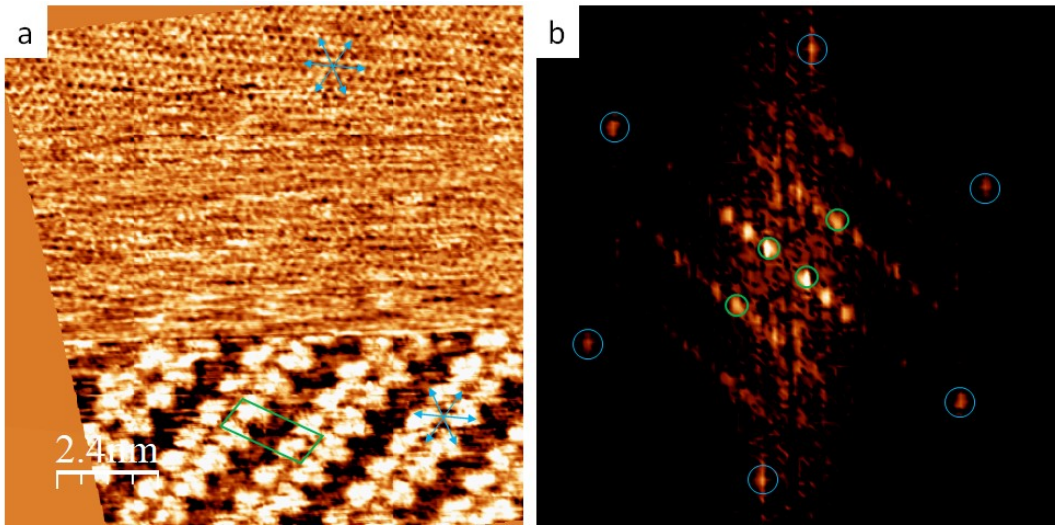

Figure S2. (a) Split STM image with resolution of the HOPG lattice (top) and the molecular lattice of DSeDPP phase II (bottom) at the 1-octanoic acid/HOPG interface. Blue arrows point at high symmetry directions of the HOPG and the molecular lattice is indicated by a green cell. (b) 2DFFT of the STM image given in (a). The blue circles represent the high symmetry directions of the HOPG lattice and the green circles represent the molecular lattice.

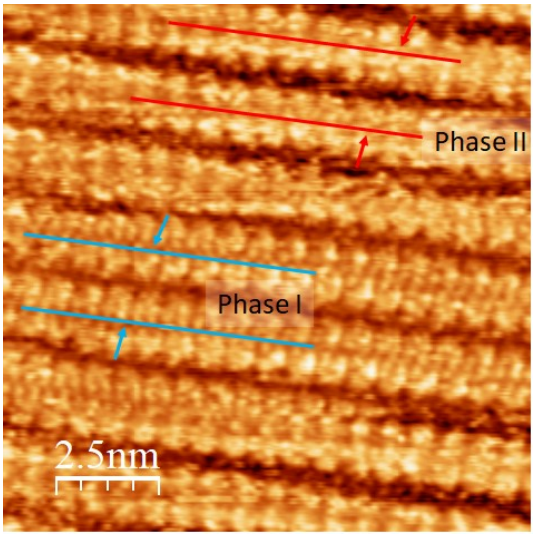

Figure S3. STM image of DSeDPP self-assembly at octanoic acid-HOPG interface showing phase I and phase II with different interlamellar spacings: 1.6 ± 0.1 nm for phase I (blue) and 2.0 ± 0.1 nm for phase II (red). U = −500 mV, I = 50 pA.

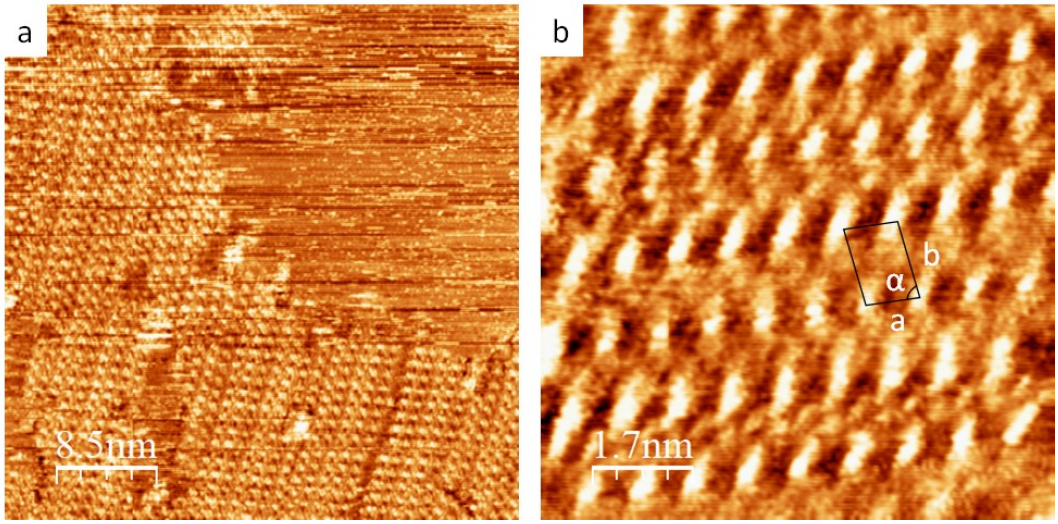

Figure S4. Large-scale (a) and detailed (b) STM images of DTzDPP self-assembly at 1,2,4-trichlorobenzene (TCB)-HOPG interface. U = −500 mV, I = 50 pA. (b) Lattice constants are a = 0.8 ± 0.1 nm, b = 1.3 ± 0.1 nm, and α = 74 ± 2°.

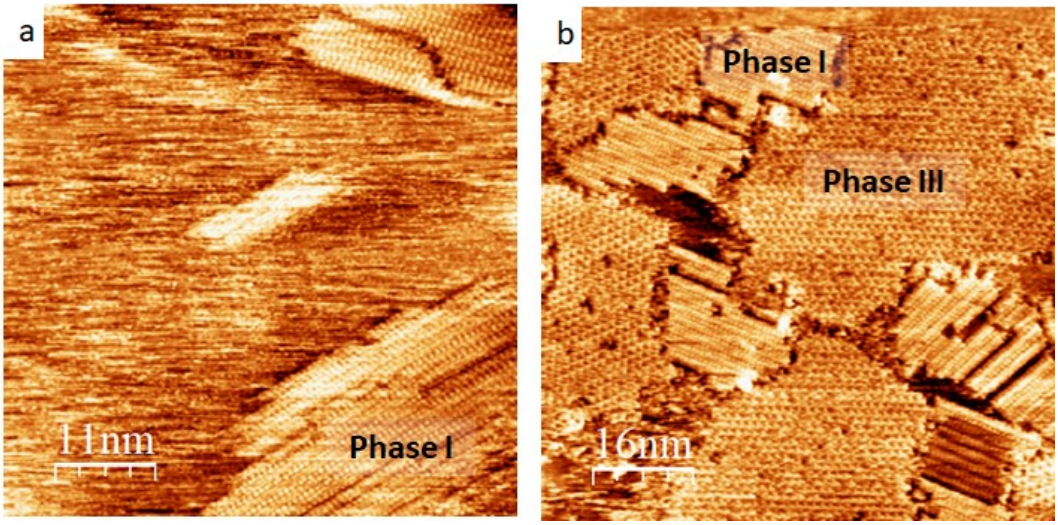

Figure S5. STM images that reveal the concentration effect in DTTDPP self-assembly at the octanoic acid-HOPG interface. The relative coverage of phase III increases with the concentration of the applied solution. The images were obtained using solutions with concentrations 4.8×10^{-4} M (a) and 4.1×10^{-3} M (b). U = −500 mV, I = 50 pA.

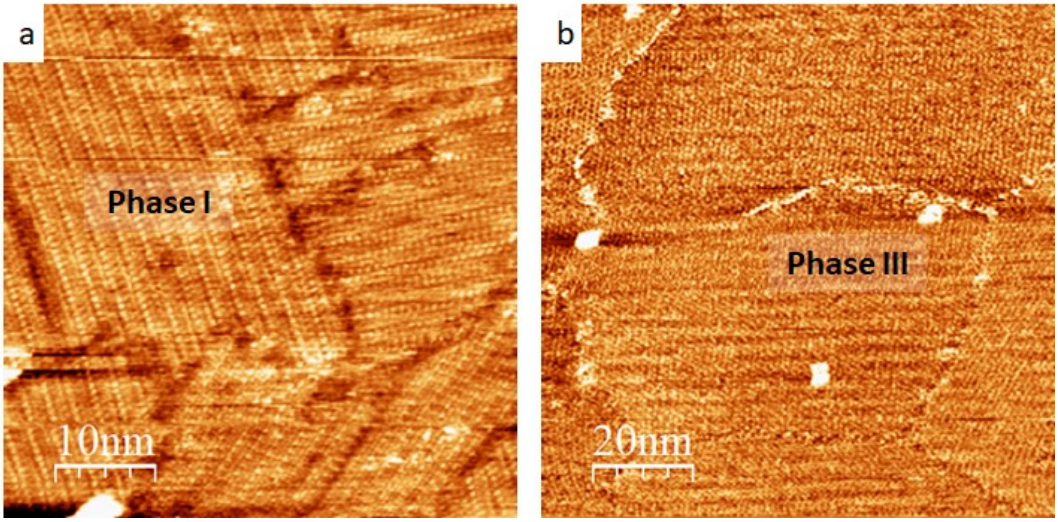

Figure S6. STM images showing the concentration effect in DTTDPP self-assembly at the TCB-HOPG interface. The relative coverage of phase III increases with the concentration. The images were obtained using solutions with concentrations 2.2×10^{-3} M (a) and 3.4×10^{-2} M (b). U = −500 mV, I = 50 pA.

3) Additional DFT simulation results

DFT simulations were performed using PBE-GGA for exchange-correlation potential and DFT-D3 for dispersion correction.

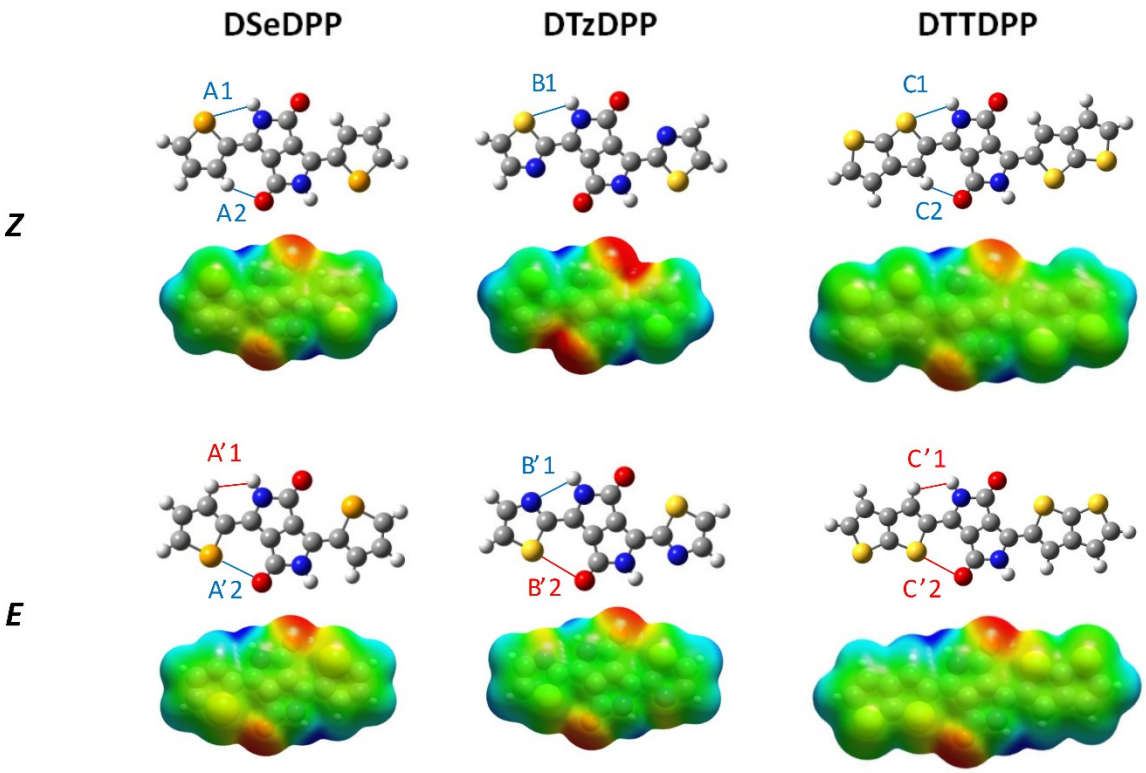

Figure S7. Electrostatic potential maps corresponding to the *Z* and *E* conformers of DSeDPP, DTzDPP, and DTTDPP (isosurface value: 0.0004, ESP extrema: −0.05 eV (red) and 0.05 eV (blue), produced in Gaussian 16 using M06-2x functional with the 6-31G(d) basis set). Close contacts are marked in each molecular model as colored lines: Blue color for attractive interactions and red color for repulsive interactions. A1 = 2.92 Å, A2 = 2.26 Å, A'1 = 2.27 Å, A'2 = 3.10 Å, B1 = 2.82 Å, B'1 = 2.58 Å, B'2 = 3.20 Å, C1 = 2.84 Å, C2 = 2.26 Å, C'1 = 2.27 Å, and C'2 = 3.09 Å.

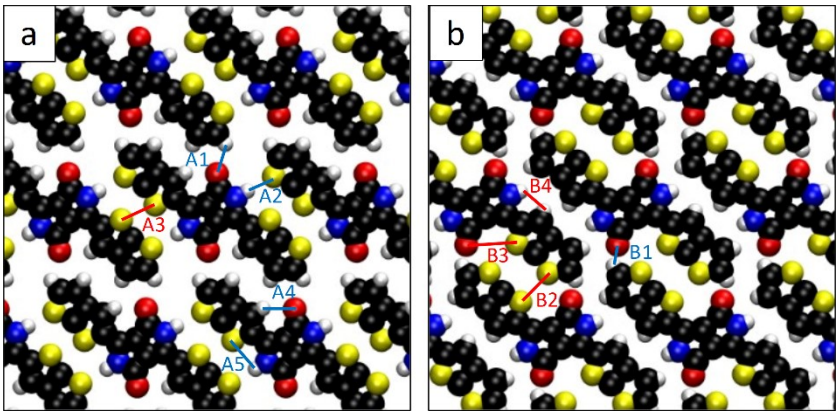

Figure S8. Lattices constructed to model the polymorph III of DTTDPP. (a) DFT-optimized lattice with (*Z*)-DTTDPP. All the inter- and intramolecular contacts are shown as colored lines with attractive interactions in blue and repulsive interactions in red. This geometry facilitates four weak H-bonding per molecule between the thienothiophene H and lactam O, and thienothiophene S and lactam H represented by intermolecular contacts A1 and A2, respectively. A1 = 2.36 Å, A2 = 2.87 Å, A3 = 3.59 Å, A4 = 2.43 Å, A5 = 2.85 Å. (b) The structure with the (*E*)-DTTDPP did not converge likely due to the lesser number of weak H-bonding and more repulsive interactions per molecule. Possible close contacts are marked with colored lines (blue and red for attractive and repulsive interactions, respectively). Only two weak H-bondings per molecule, between thienothiophene H and lactam O are possible in this case (B1).

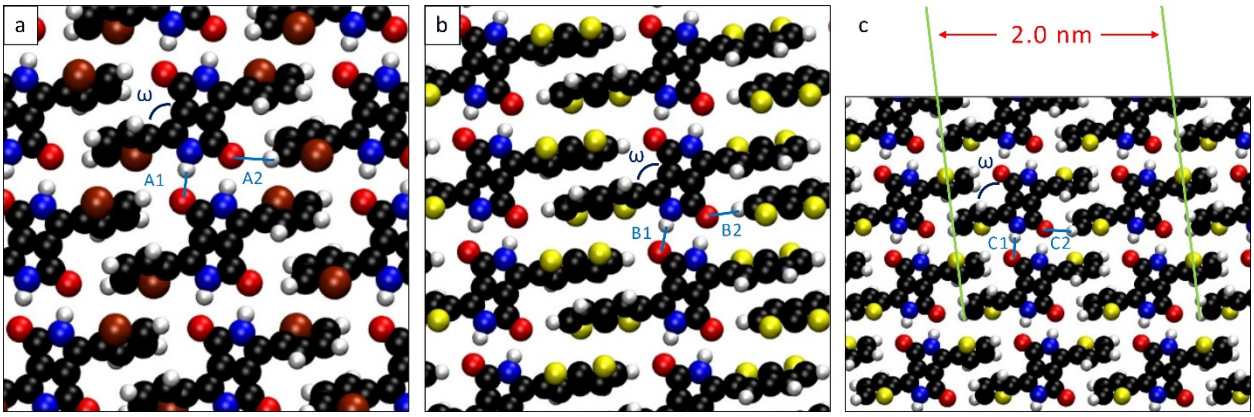

Figure S9. DFT-optimized structures of the homoassemblies corresponding to DSeDPP (a), DTTDPP (b), and DTDPP (c) with substituent rings twisted out-of-plane. Blue lines represent attractive interactions in the assemblies: A1 = 1.80 Å, A2 = 2.49 Å, B1 = 1.77 Å, B2 = 2.26 Å, C1 = 1.80 Å, and C2 = 2.49 Å. The dihedral angles corresponding to the rotation of the aromatic ring (ω) are ~57° for DSeDPP, ~63° for DTTDPP, and ~56° for DTDPP. (c) The periodicity of the protruding S atoms is 2.0 nm and the H-bonded molecules within a lamella have a periodicity of 0.7 nm.

The energy profiles of dihedral rotation (**Figure S10**) were carried out employing the climbing-image NEB method in VASP with a pathway divided into eight intermediate images of DPP molecules corresponding to dihedral angles between 0° and 180° for *one* DPP-aryl inter-ring bond (PBE-GGA functional with DFT-D3 vdW correction). This shows almost the same trend as the conformational preference obtained using M06-2X functional in Gaussian (**Figure 4** in the MS).

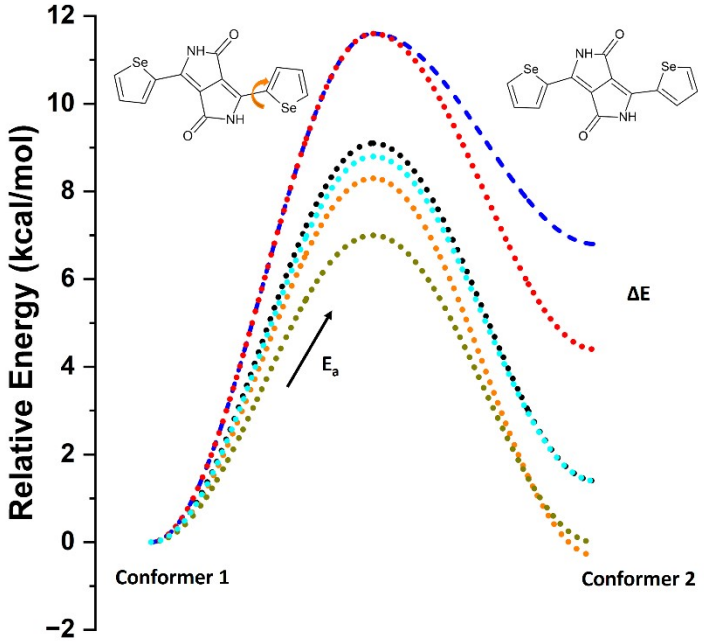

Molecule	Conformer 1	Conformer 2	E_a (kcal/mol)	ΔE (kcal/mol)
DPDPP	N/A	N/A	7.0	0.0
DFDPP	(*Z*, *Z*)	(*Z*, *E*)	11.6	4.4
DTDPP	(*Z*, *Z*)	(*Z*, *E*)	8.8	1.4
DSeDPP	(*Z*, *Z*)	(*Z*, *E*)	8.3	−0.3
DTzDPP	(*E*, *E*)	(*E*, *Z*)	11.6	6.8
DTTDPP	(*Z*, *Z*)	(*Z*, *E*)	9.1	1.4

Figure S10. The plot shows the energy barriers (E_a) for the dihedral rotation around the carbon-carbon bond between the DPP backbone and *one* aryl substituent, and the enthalpy changes (ΔE) between the corresponding conformers of the DPP precursors imaged in this work and previous work by Fu *et al.*[1] ΔE and E_a are calculated between (*Z*, *E*) and (*Z*, *Z*) conformers except for DTzDPP, where the energy values are calculated between (*E*, *Z*) and (*E*, *E*) conformers. The energy values are given in the table (right side), which are calculated using the nudged elastic band (NEB) method in VASP (PBE-GGA functional with DFT-D3 vdW correction).

Table S1. The energy differences between *E* and *Z* conformers of DPP molecules (dE) and the adsorption energies of *Z* and *E* conformers of DPP molecules on graphene (E_{Ads}^{Mol}).

Molecule	dE (kcal/mol)	E_{Ads}^{Mol} of *Z* conformer (kcal/mol)	E_{Ads}^{Mol} of *E* conformer (kcal/mol)
DSeDPP	-0.5	-29.1	-28.9
DTzDPP	-13.8	-28.2	-27.6
DTTDPP	2.9	-36.6	-36.8

The energy values are calculated using VASP with PBE-GGA functional and DFT-D3 vdW correction. *E* conformer is more stable than *Z* conformer by **0.5 kcal/mol** for **DSeDPP**, *E* conformer is more stable than *Z* conformer by **13.8 kcal/mol** for **DTzDPP**, and *Z* conformer is more stable than *E* conformer by **2.9 kcal/mol** for **DTTDPP**.

Adsorption energy calculations were performed using the equation:

$$E_{Ads}^{Mol} = E_{Mol + Graphene} - E_{Mol} - E_{Graphene}$$

The adsorption energy calculations were performed by placing the molecules along the zigzag axis of the graphene. We also looked at the variation in E_{Ads}^{Mol} of molecules with adsorption sites (top, bridge, and hollow) and orientation on graphene, where significant variations were not found. For instance, **Figure S11** depicts the E_{Ads}^{Mol} of DSeDPP (*E* conformer) when adsorbed at different adsorption sites of graphene and different orientations with respect to the graphene, which shows that E_{Ads}^{Mol} variations are less than 0.3 kcal/mol for DSeDPP. Therefore, the choice of the adsorption site of the molecule or molecular orientation on graphene does not have a significant effect on the value of E_{Ads}^{Mol}.

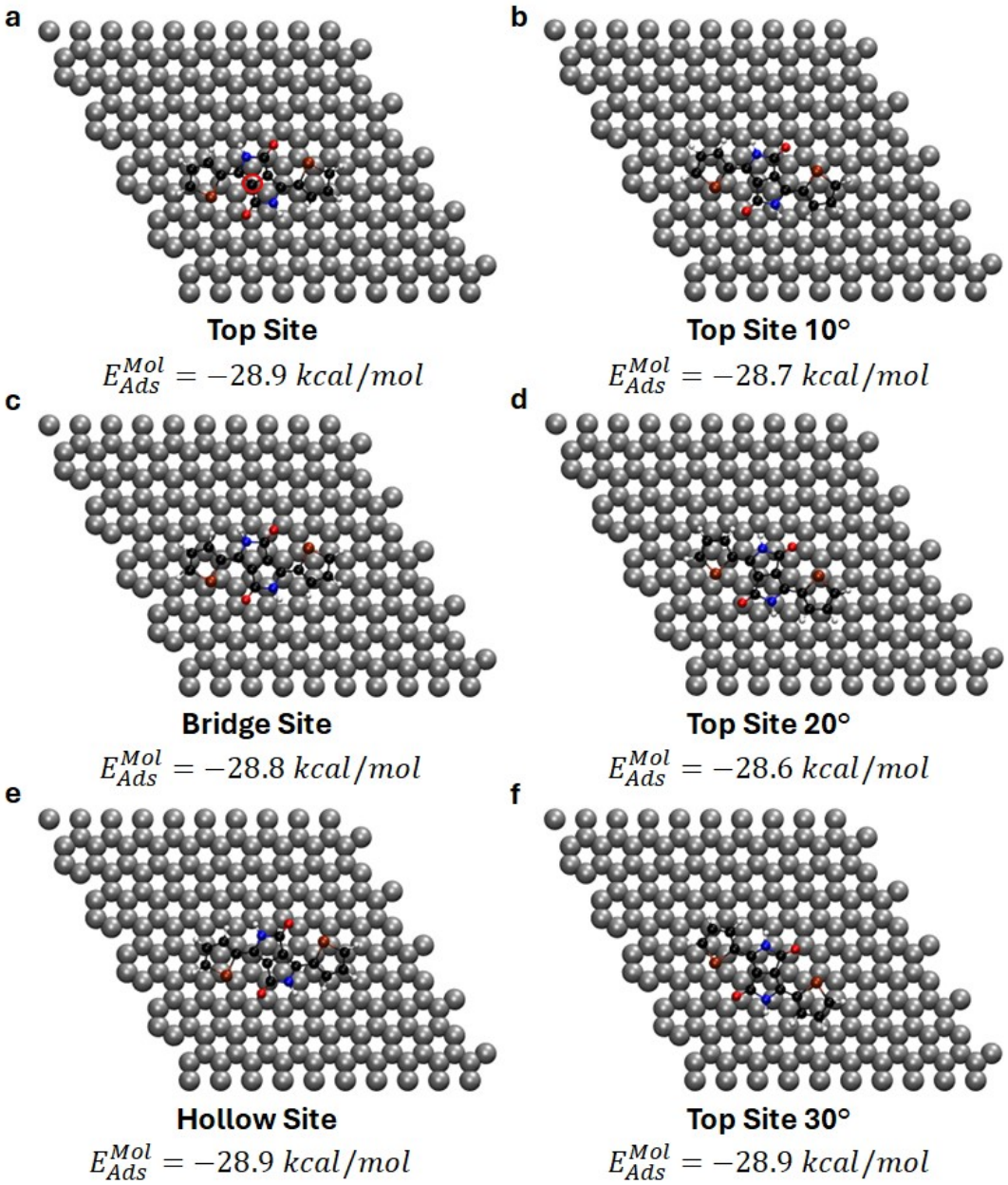

Figure S11. Variation in adsorption energy (E_{Ads}^{Mol}) of (*E*)-DSeDPP with adsorption sites or orientation on graphene. The red circle in (a) represents the carbon atom that is used to define the molecule's adsorption site on graphene. The adsorption energy corresponding to each geometry is given below the image. The adsorption energy variations with adsorption sites (a, c, e) and orientation of the molecule (a, b, d, f) on graphene are less than 0.3 kcal/mol. DSeDPP molecules in (a), (c), and (e) are aligned along the zigzag axis of graphene. DSeDPP molecules in (b), (d), and (f) are 10°, 20°, and 30° rotated with respect to the zigzag axis of graphene, respectively.

4) Synthesis of DPP precursors

Thieno[2,3-*b*]thiophene was synthesized according to an adaptation of published procedures.[2,3] Malononitrile, ethyl bromoacetate and selenophene were purchased from Sigma-Aldrich. Chlorosulfonyl isocyanate and diisopropyl succinate were purchased from TCI. *t*-Amyl alcohol was purchased from Fisher Scientific. **DTzDPP** was purchased from 1-Material Inc. All reagents were used without further purification.

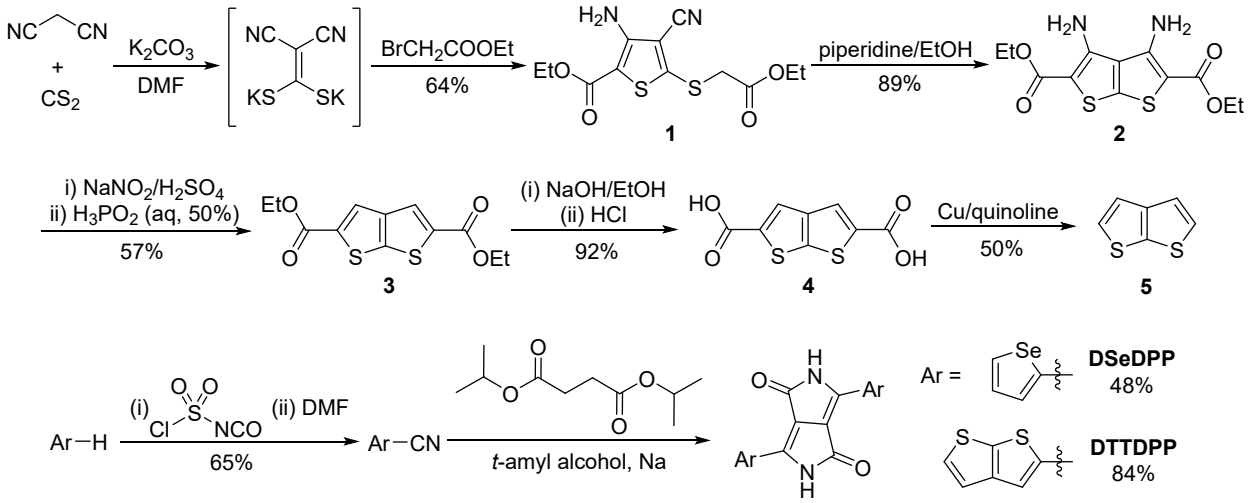

Scheme S1. Reactions that were carried out to synthesize DSeDPP and DTTDPP.

Ethyl 3-amino-4-cyano-5-(2-ethoxy-2-oxethylthio)thiophene-2-carboxylate (**1**): To a solution of malononitrile (6.673 g, 0.101 mol) in 40 mL DMF was added anhydrous K_2CO_3 (41.46 g, 0.300 mol) under argon, followed by CS_2 (11.42 g, 0.150 mol) dropwise through an addition funnel upon vigorous stirring. The mixture was stirred for 30 min and then cooled on an ice bath. A solution of ethyl bromoacetate (33.4 g, 0.20 mol) in 10 mL DMF was added dropwise. The mixture was stirred overnight at room temperature and poured into ~200 mL cold water. The precipitate was filtered, washed with water and air-dried to give a gold solid (20.339 g, 64%). ^{1}H NMR (300 MHz, $CDCl_3$): 5.78 (br, 2H), 4.33 - 4.21 (m, 4H), 3.78 (s, 2H), 1.36 -1.27 (m, 6H). ^{13}C NMR (75 MHz, $CDCl_3$): 167.66, 162.88, 153.16, 151.71, 112.53, 103.99, 62.61, 61.06, 38.09, 14.61, 14.25.

Diethyl 3,4-diaminothieno[2,3-b]thiophene-2,5-dicarboxylate (**2**): A solution of **1** (19.17 g, 61.0 mmol) in 60 mL EtOH and 0.6 mL piperidine was refluxed for several hours. The reaction mixture was cooled and the solid was filtered (16.97 g, 89%). ^{1}H NMR (300 MHz, DMSO-d_6): 7.11 (br, 4H), 4.21 (q, 4H, J = 7.2 Hz), 1.25 (t, 6H, J = 7.2 Hz). ^{13}C NMR (75 MHz, DMSO-d_6): 163.53, 148.65, 147.19, 127.91, 98.44, 59.61, 14.45.

Diethyl thieno[2,3-b]thiophene-2,5-dicarboxylate (**3**): To 80 mL H_2SO_4 (75%) in a three-necked round bottom flask was added **2** (5.0 g, 16 mmol) while stirring. Upon formation of the ammonium salt, the slurry was cooled to 2−3 ˚C and 16 mL aqueous $NaNO_2$ (2.3 M) was added dropwise. The mixture was stirred until all the solid dissolved (~1.5 h). The cold solution was transferred to a dropping funnel and added to 80 mL aqueous H_3PO_2 (50%) under vigorous stirring. After stirring overnight, the precipitate was filtered and washed with water until neutral to give an ochre powder (2.60 g, 57%). ^{1}H NMR (300 MHz, $CDCl_3$): 7.95 (s, 2H), 4.39 (q, 4H, J = 6.9 Hz), 1.40 (t, 6H, J = 7.2 Hz). ^{13}C NMR (75 MHz, $CDCl_3$): 162.05, 148.10, 145.31, 137.77, 126.80, 61.83, 14.50.

Thieno[2,3-b]thiophene-2,5-dicarboxylic acid (**4**): A solution of **3** (7.30 g, 25.7 mmol) and NaOH (4.10 g, 0.103 mol) in 250 mL EtOH was refluxed for 6 h. The solution was cooled, acidified with aqueous HCl and filtered to give the title compound (92%). ^{1}H NMR (300 MHz, DMSO-d_6): 13.40 (br, 2H), 7.98 (s, 2H). ^{13}C NMR (75 MHz, DMSO-d_6): 162.95, 147.13, 145.18, 138.43, 126.82.

Thieno[2,3-b]thiophene (**5**): A suspension of **4** (0.722 g, 3.16 mmol) and copper (0.191 g, 3.01 mmol) in 6 mL freshly distilled quinoline was refluxed for 1 h. The cooled reaction mixture was extracted with petroleum ether. The organic layer was washed with 2 M HCl (3×30 mL) and brine (3×50 mL), dried over $MgSO_4$ and concentrated to give a colorless oil (0.222 g, 50%). ^{1}H NMR (400 MHz, $CDCl_3$): 7.36 (d, 2H, J = 5.2 Hz), 7.25 (d, 2H, J = 5.2 Hz). ^{13}C NMR (75 MHz, $CDCl_3$): 147.19, 137.48, 128.36, 119.97.

Thieno[2,3-b]thiophene-2-carbonitrile: To a solution of **5** (1.446 g, 10.3 mmol) in 6 mL anhydrous DCM was slowly added chlorosulfonyl isocyanate (2.00 mL, 23.0 mmol) under nitrogen. The mixture was stirred at room temperature for 3 h. To the mixture was added DMF (4 mL) and stirring was continued for 1 h. The mixture was poured into water, extracted with DCM, dried over $MgSO_4$, concentrated and purified by flash chromatography (10% DCM in hexanes) to give an off-white solid (1.115 g, 65%). ^{1}H NMR (500 MHz, $CDCl_3$): 7.77 (s, 1H), 7.51 (d, 1H, J = 5.3 Hz), 7.29 (d, 1H, J = 5.3 Hz). ^{13}C NMR (500 MHz, $CDCl_3$): 145.53, 142.77, 130.98, 130.27, 120.32, 114.51, 111.72.

Selenophene-2-carbonitrile: To a solution of selenophene (0.663 g, 5.1 mmol) in 5 mL anhydrous DCM was slowly added chlorosulfonyl isocyanate (1.00 mL, 11.5 mmol) under nitrogen. The mixture was stirred at room temperature for 2 h. To the mixture was added DMF (2 mL) and stirring was continued for 1 h. The mixture was poured into water, extracted with DCM, dried over $MgSO_4$, concentrated and purified by flash chromatography (5% EtOAc in hexanes) to give a slightly yellowish oil (0.510 g, 65%). ^{1}H NMR (500 MHz, $CDCl_3$): 8.36 (dd, 1H, J = 5.5 Hz, J' = 1.2 Hz), 7.88 (dd, 1H, J = 3.9 Hz, J' = 1.2 Hz), 7.37 (dd, 1H, J = 5.5 Hz, J' = 3.9 Hz).

3,6-Di(selenophen-2-yl)-2,5-dihydropyrrolo[3,4-c]pyrrole-1,4-dione (**DSeDPP**): Sodium (0.145 g, 6.31 mmol) was refluxed in 6 mL *t*-amyl alcohol under nitrogen until fully reacted. Selenophene-2-carbonitrile (0.493 g, 3.16 mmol) and diisopropyl succinate (0.342 g, 1.69 mmol) were added and the mixture was stirred at 85 ˚C overnight under nitrogen. The mixture was cooled to 50 ˚C, quenched with 0.4 mL AcOH in 5 mL MeOH and stirred for 30 min. The dark green solid was filtered, washed with MeOH and acetone and dried in vacuum (0.297 g, 48%). ^{1}H NMR (500 MHz, DMSO-d_6): 11.23 (s, 2H), 8.61 (dd, 2H, J = 5.5 Hz, J' = 1.1 Hz), 8.32 (dd, 2H, J = 4.0 Hz, J' = 1.1 Hz), 7.50 (dd, 2H, J = 5.5 Hz, J' = 3.9 Hz).

3,6-Di(thieno[2,3-b]thiophen-2-yl)-2,5-dihydropyrrolo[3,4-c]pyrrole-1,4-dione (**DTTDPP**): Sodium (0.212 g, 9.22 mmol) was refluxed in 10 mL *t*-amyl alcohol under nitrogen until fully reacted. Thieno[2,3-*b*]thiophene-2-carbonitrile (0.842 g, 5.10 mmol) and diisopropyl succinate (0.523 g, 2.59 mmol) were added and the mixture was stirred at 100 ˚C for 48 h under nitrogen. The mixture was cooled to 50 ˚C, quenched with 0.6 mL AcOH in 4 mL MeOH and stirred for 30 min. The dark red solid was filtered, washed with MeOH and acetone and dried in vacuum (0.887 g, 84%). ^{1}H NMR (500 MHz, DMSO-d_6): 11.37 (s, 2H), 8.37 (s, 2H), 7.74 (d, 2H, J = 5.3 Hz), 7.46 (d, 2H, J = 5.3 Hz).

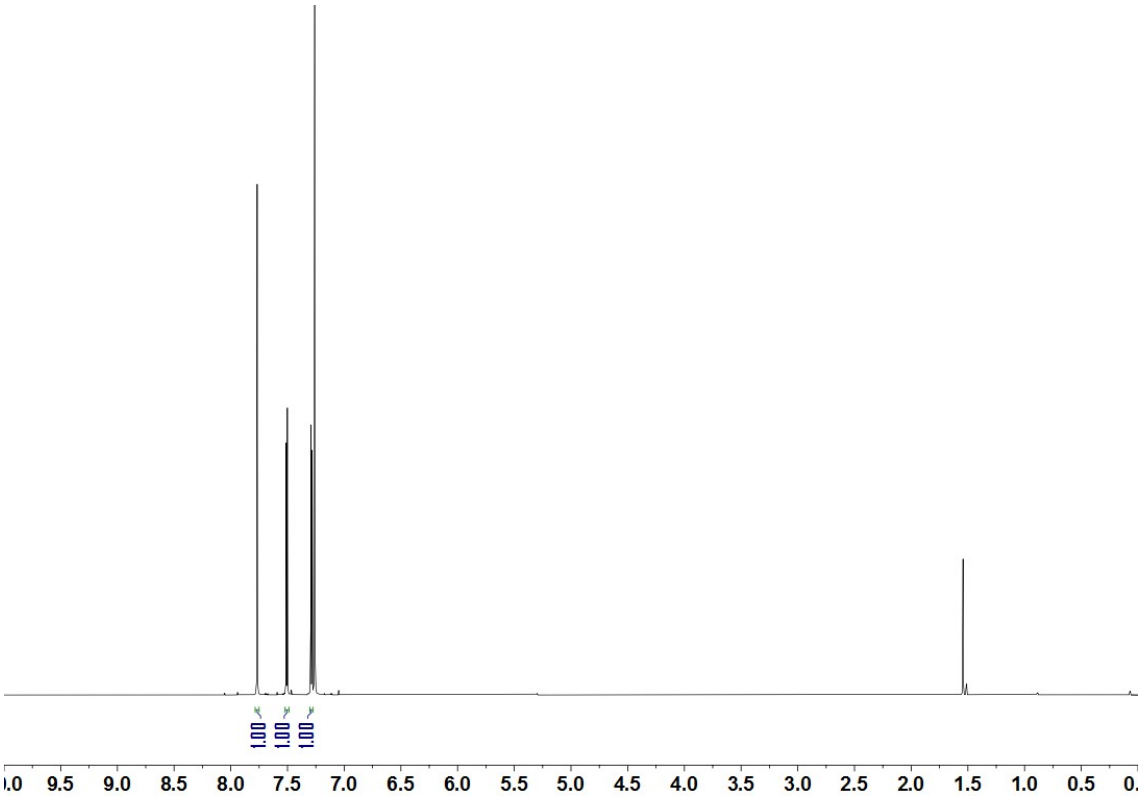

Figure S12. ^{1}H NMR (500 MHz, $CDCl_3$) of thieno[2,3-*b*]thiophene-2-carbonitrile.

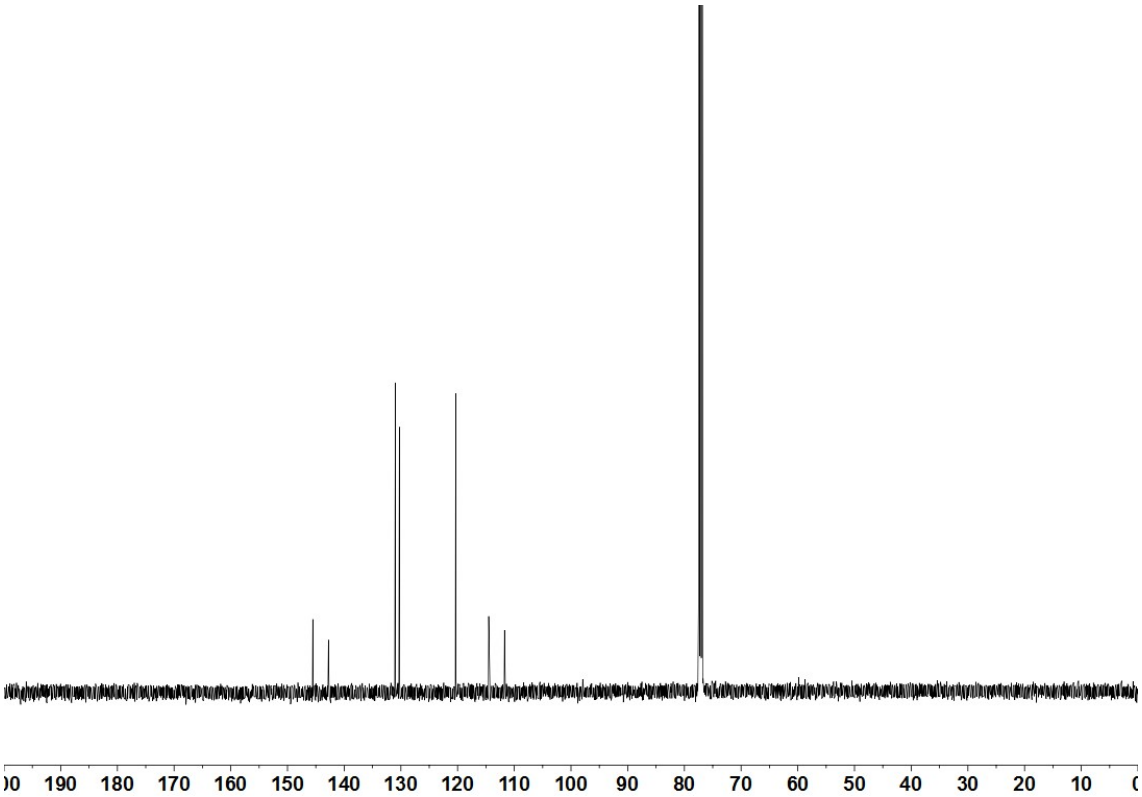

Figure S13. ^{13}C NMR (500 MHz, $CDCl_3$) of thieno[2,3-*b*]thiophene-2-carbonitrile.

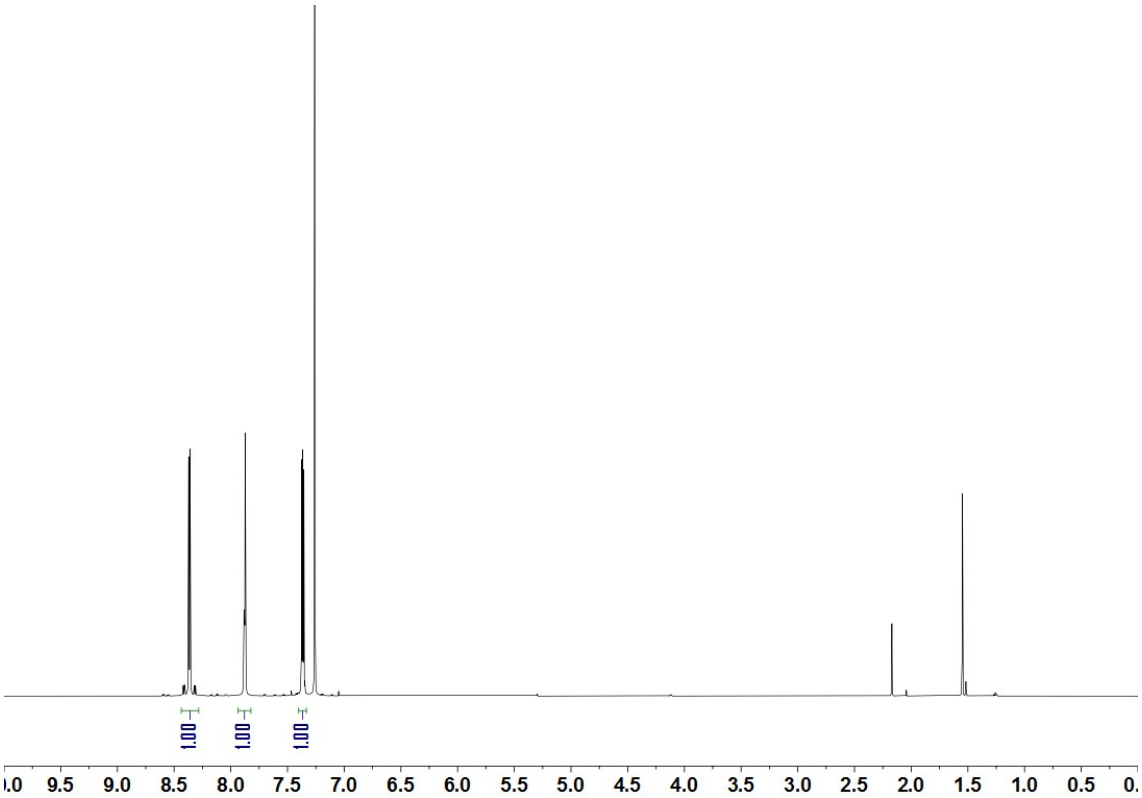

Figure S14. ^{1}H NMR (500 MHz, $CDCl_3$) of selenophene-2-carbonitrile.

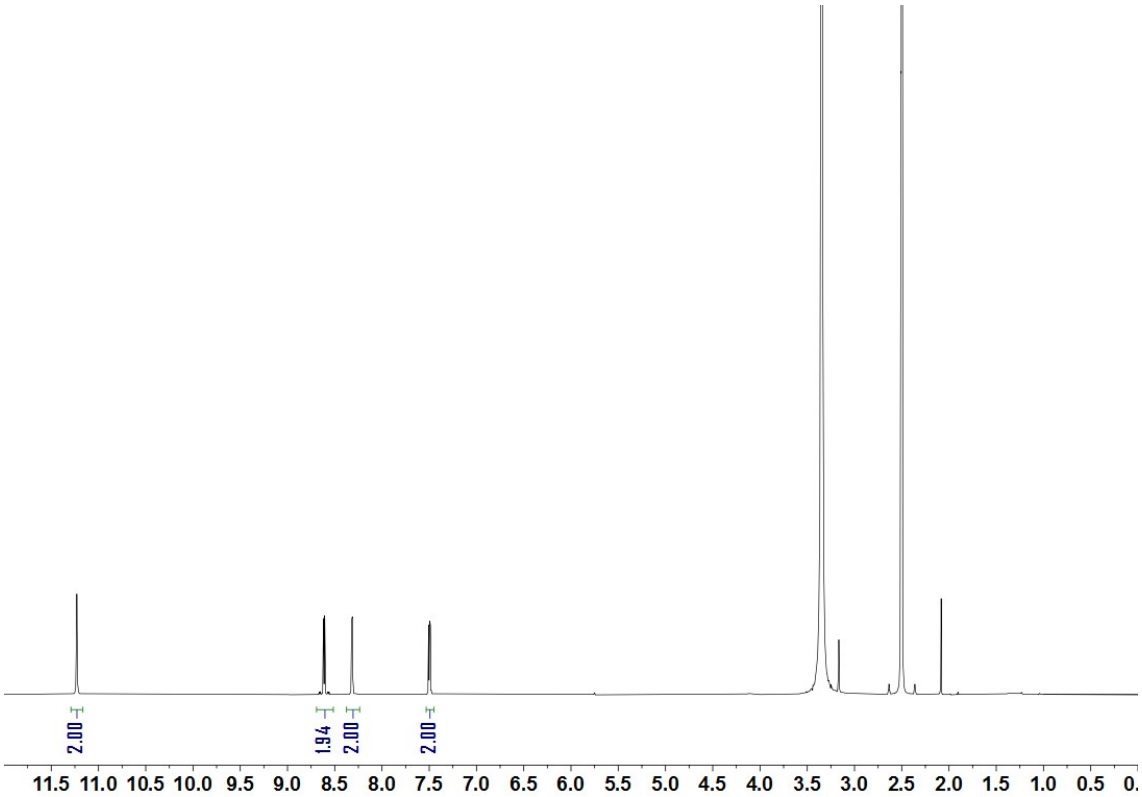

Figure S15. ^{1}H NMR (500 MHz, DMSO-d_6) of **DSeDPP**.

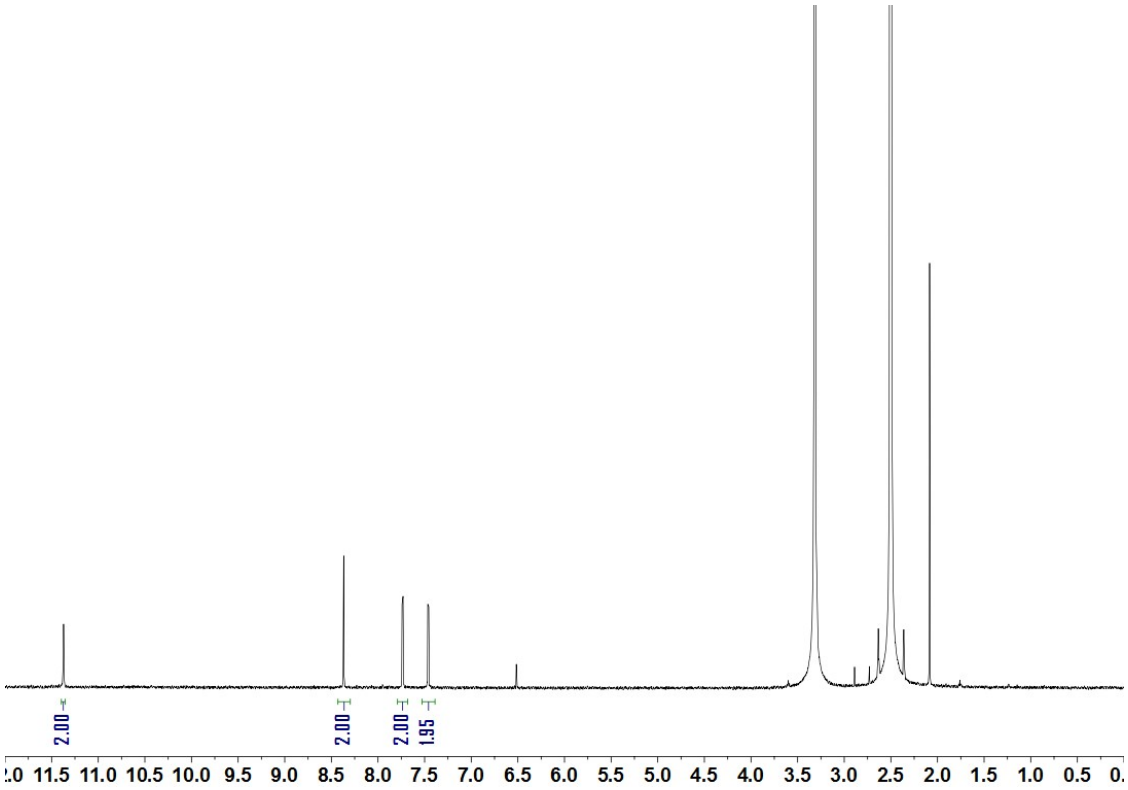

Figure S16. ^{1}H NMR (500 MHz, DMSO-d_6) of **DTTDPP**.

References

1 C. Fu, P. J. Beldon and D. F. Perepichka, *Chem. Mater.*, 2017, **29**, 2979–2987.
2 A. Cornel and G. Kirsch, *J. Heterocycl. Chem.*, 2001, **38**, 1167–1171.
3 A. K. El-shafei, H. A. Abdel-ghany, A. A. Sultan and A. M. M. El-saghier, *Phosphorus Sulfur Silicon Relat. Elem.*, 1992, **73**, 15–25.